

Aryl C(sp²)-X Coupling (X = C, N, O, Cl) and Facile Control of N-Mono- and N,N-Diarylation of Primary Alkylamines at a Pt(IV) Center

Xiaoxi Lin, Arkadi Vigalok,* and Andrei N. Vedernikov*

Cite This: *J. Am. Chem. Soc.* 2020, 142, 20725–20734

Read Online

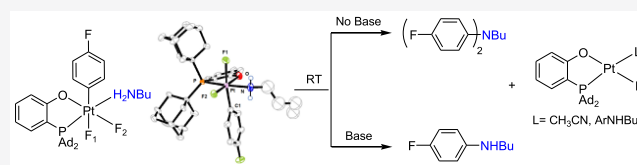
ACCESS |

Metrics & More

Article Recommendations

Supporting Information

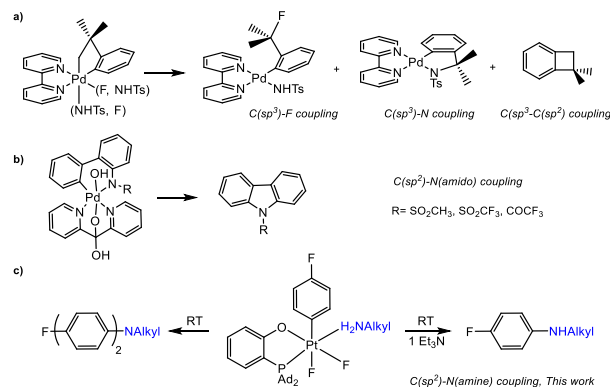
ABSTRACT: We present the first example of an unprecedented and fast aryl C(sp²)-X reductive elimination from a series of isolated Pt(IV) aryl complexes (Ar = *p*-FC₆H₄) LPt^{IV}F(py)(Ar)X (X = CN, Cl, 4-OC₆H₄NO₂) and LPt^{IV}F₂(Ar)(HX) (X = NHalk; Alk = *n*-Bu, PhCH₂, cyclo-C₆H₁₁, *t*-Bu, cyclopropylmethyl) bearing a bulky bidentate 2-[bis(adamant-1-yl)phosphino]phenoxide ligand (L). The C(sp²)-X reductive elimination reactions of all isolated Pt(IV) complexes follow first-order kinetics and were modeled using density functional theory (DFT) calculations. When a difluoro complex LPt^{IV}F₂(Ar)(py) is treated with TMS-X (TMS = trimethylsilyl; X = NMe₂, SPh, OPh, CPh) it also gives the corresponding products of the Ar-X coupling but without observable LPt^{IV}F(py)(Ar)X intermediates. Remarkably, the LPt^{IV}F₂(Ar)(HX) complexes with alkylamine ligands (HX = NH₂Alk) form selectively either mono- (ArNHalk) or diarylated (Ar₂Nalk) products in the presence or absence of an added Et₃N, respectively. This method allows for a one-pot preparation of diarylalkylamine bearing different aryl groups. These findings were also applied in unprecedented mono- and di-N-arylation of amino acid derivatives (lysine and tryptophan) under very mild conditions.



1. INTRODUCTION

The formation of the new C-X (X = C, heteroatom) bonds via reductive elimination from a group 10 M(IV) atom is the product-forming step in a variety of catalytic oxidative transformations that have attracted much attention in the last two decades.^{1,2} As compared to the more common M(II) counterparts, high-valent d⁶ metal complexes have a greater number of donor atoms at the metal center, which may imply greater competitiveness when it comes to the C-X bond formation and, hence, may require more careful control over the reaction selectivity.³ For example, a competitive formation of C(sp³)-N, C(sp³)-F, and C(sp³)-C(sp²) bonds can be observed at a Pd(IV) center in a single complex (Scheme 1a), as has been reported by Sanford and co-workers.⁴ Notably, a preference for the C(sp³)-X vs C(sp²)-X reductive elimination is typical for this and similar systems.⁵ As a result of significant efforts targeting isolation and characterization of various Pd(IV) and, more recently, Ni(IV) organometallic derivatives exhibiting clean C-X bond reductive elimination reactivity,¹ this chemistry is now well-established, although some “blind spots” remain. As a consequence, the intermediacy of organopalladium(IV) species is now routinely proposed in various palladium-catalyzed C-X coupling reactions performed under sufficiently oxidizing conditions.⁶ In turn, thanks to a greater kinetic inertness,⁷ Pt(IV) complexes can serve a better role as models to study some still poorly characterized C-X bond coupling reactions.^{3,8–11} Surprisingly, in spite of some notable progress in this field, a number of aryl C(sp²)-X

Scheme 1. C-N Elimination from a M(IV) Center



coupling reactions involving well-characterized isolable Pt(IV) compounds (e.g., for X = Cl, O, N) have never been observed.¹²

Focusing specifically on a C-N bond formation at a M(IV) center, most of the accomplished research deals with the

Received: September 2, 2020

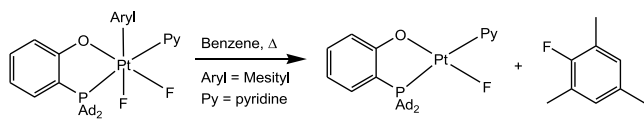
Published: November 23, 2020



C(sp³)-N coupling involving an S_N2 attack at the metal-bound alkyl groups lacking β-hydrogen atoms.^{1c,10c,13} In turn, stabilized amide anions are typically employed as coupling partners combining accessibility, chemical robustness, and appreciable reactivity as nucleophile.^{1,4,10,11,13,14} While many catalytic C(sp²)-N coupling reactions were proposed to proceed via putative Pd(IV) intermediates, in none of the cases were such intermediates characterized.^{6b} Only one report of a well-characterized C(sp²)-N(sulfonyl, acyl) coupling of isolated Pd(IV) amido aryl complexes has recently been published by one of us (Scheme 1b).¹⁵ In turn, to the best of our knowledge, no C(sp²)-N(hydrocarbyl) reductive coupling reactions of any isolable group 10 M(IV) amines complexes have been characterized so far. Considering the importance of metal-catalyzed and metal-mediated N-mono- and N,N-diarylation, especially in the synthesis of biologically active compounds,^{16,17} we report here the preparation of aryl Pt(IV) complexes with a series of alkylamines, as well as experimental and computational characterization of their unusually facile aryl C(sp²)-N(Alk) reductive elimination reactivity. By merely changing the basicity of the system, selective and high-yielding mono- or diarylation of the coordinated amine can be achieved (Scheme 1c). The developed approach has been used for an unprecedented mono- and di-NH-arylation of partially protected lysine and tryptophan under very mild conditions.

Recently, we presented the first example of a highly selective aryl-F reductive elimination reaction from an isolated Pt(IV) aryloxo fluoro complex (Scheme 2).⁸ Notably, similar

Scheme 2. Aryl-F Elimination from a Pt(IV) Center

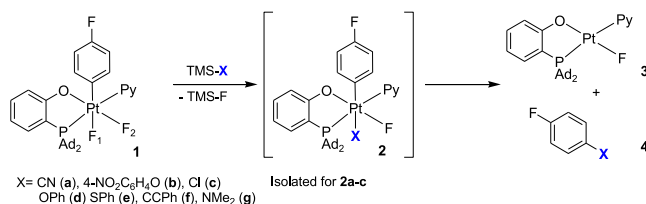


reactions involving heavier halogens, Br and I, are easier to observe.⁹ We proposed that the exclusive C-F bond formation was sterically enforced by the presence of the bulky mesityl and 2-[bis(adamant-1-yl)phosphino]phenoxide (P-O) ligands. Thus, this ligand scaffold might also be efficient for enabling other difficult aryl-X elimination reactions (e.g., X = Cl, CN, O, N(alkyl)) at a Pt(IV) center, hopefully in a selective manner.

2. RESULTS AND DISCUSSION

2.1. *p*-FC₆H₄-X Elimination from Pt(IV) Aryl Complexes. The target aryl (P-O)Pt(IV) precursors **2a** (X = CN), **2b** (X = 4-OC₆H₄NO₂), and **2c** (X = Cl) have been prepared using Pt(IV) aryl difluoride **1** and an appropriate TMS-X reagent at room temperature (Scheme 3), isolated,

Scheme 3. Selective Ar-X Reductive Elimination at a Pt(IV) Center



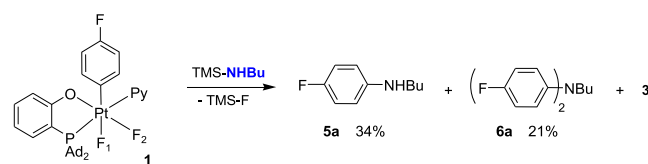
and fully characterized.¹⁸ Notably, the *p*-nitrophenoxo complex **2b** has been characterized by single-crystal X-ray diffraction (Figure S1), confirming that the reaction of **1** with TMS-4-OC₆H₄NO₂ led to the selective replacement of the fluoride ligand F_a, trans to the aryl, giving the product with the mutual trans arrangement of the aryl and 4-nitrophenoxo groups. The remaining fluoride ligand F_b showed the characteristic upfield (below -300 ppm) ¹⁹F NMR signals for all three complexes, thus revealing the same diastereoselectivity of these ligand substitution reactions. Analogous compounds **2d** (X = OPh), **2e** (X = SPh), **2f** (X = CPh), and **2g** (X = NMe₂) were not detected by NMR spectroscopy when **1** and the corresponding TMS-X reagents were reacted either at room temperature (**4e,g**) or upon heating to 65 °C (**4d,f**). Instead, the formations of Ar-X coupling products **4d-4g**, along with TMS-F and the corresponding Pt(II) complex **3**, were observed, thus suggesting that, for **1d-1g**, the C-X reductive elimination reactions from transient **2d-2g** are faster than the formation of complexes **2** from **1** and the corresponding TMS-X.

The isolated Pt(IV) cyanide **2a** demonstrated the formation of Ar-CN product following a clean first-order kinetics in EtCN solutions ($k_{353K} = 3.41 \pm 0.44 \times 10^{-4} \text{ s}^{-1}$, $\Delta G^\ddagger = 26.5 \text{ kcal/mol}$, Figure S2) and could be produced in ca. 70% yield after 1.5 h at 80 °C. The reaction was only slightly slowed by the presence of 10 equiv of pyridine ($k_{353K} = 1.21 \pm 0.01 \times 10^{-4} \text{ s}^{-1}$, $\Delta G^\ddagger = 27.2 \text{ kcal/mol}$), thus suggesting that the pyridine dissociation step is virtually irreversible in this Ar-CN coupling reaction. Both the 4-nitrophenoxo (**2b**) and the chloro (**2c**) analogues were engaged in similar transformations to form the corresponding Ar-X coupled derivatives **4b** and **4c** in 38% and 83% yields, respectively.¹⁸ Notably, neither Ar-O nor Ar-Cl coupling at a Pt(IV) center have been documented before. Our observation of the elimination of the Ar-X coupled products **4b** and **4c** pushes the limits of possible applications of aryl Pt(IV) complexes for the Ar-X bond formation and provides one with an opportunity to learn more about such reactions.

2.2. *p*-FC₆H₄-N Coupling Reactions with Primary Alkylamines. As no examples of C(sp²)-N(Alk) elimination have been reported at a *d*⁶ metal center before this work, to the best of our knowledge, we decided to explore in more detail the formation of Ar-N coupled products such as **4g** where no Pt(IV) intermediates were detected by the NMR spectroscopy (Scheme 3). When a TMS derivative of a primary alkylamine, TMS-NHⁿBu, was used in the reaction with complex **1**, the aniline **5a** formed in 34% yield at room temperature overnight (Scheme 4). Unexpectedly, the reaction was accompanied by the accumulation of significant (21% yield)¹⁹ amounts of the diarylamine (4-FC₆H₄)₂NBu, **6a** (Scheme 4).

To check if the reaction may be stepwise and **5a** can be involved in another arylation with **1**, an authentic sample of **5a** was combined with **1** to lead to a quantitative formation of **6a** within 1 h at room temperature. Thus, the reaction between **5a**

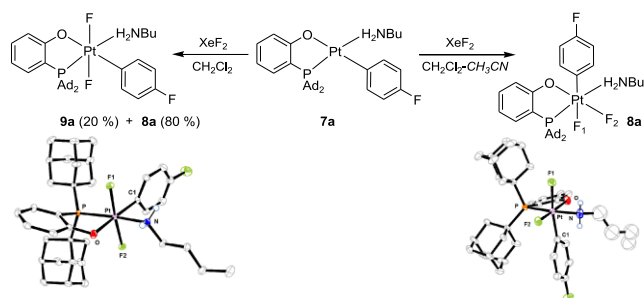
Scheme 4. Formation of N-Mono- and N,N-Diarylation Products in the Reaction of 1 with TMS-NHⁿBu



and **1** to give **6a** appears to be faster than the F-for-NHⁿBu exchange between **1** and TMS–NHⁿBu and subsequent elimination of **5a**.

Assuming that the reaction in Scheme 4 may have involved a highly reactive Pt(IV) alkylamido aryl intermediate, we sought to prepare an expectedly more robust Pt(IV) analogue containing coordinated alkylamine (P–O)Pt^{IV}F₂(*p*-FC₆H₄)(NH₂ⁿBu), **8a**. To that end, (P–O)Pt^{III}(*p*-FC₆H₄)(NH₂ⁿBu), **7a**, was reacted with XeF₂. Performing the reaction in a CH₂Cl₂–CH₃CN mixture afforded the new moderately stable Pt(IV) complex **8a** in 74% isolated yield. Complex **8a** was structurally characterized by single-crystal X-ray diffraction (Scheme 5) and was shown to be an analogue of complex **1**,

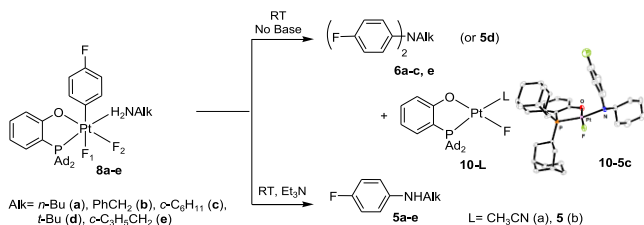
Scheme 5. Synthesis of Pt(IV) *n*-Butylamine Complexes **8a** and **9a**



with H₂NⁿBu in place of the pyridine as a ligand. The *n*-butyl fragment in the complex is severely disordered and could not be modeled reliably by discrete atoms with realistic thermal parameters. When the same reaction of complex **7a** and XeF₂ was performed in neat CH₂Cl₂, a 4:1 mixture of **8a** and the *trans*-difluoride **9a** was formed that was isolated and characterized by X-ray diffraction (Scheme 5).

Complex **9a** showed no Ar–N coupling reactivity even when heated at 50 °C in a CH₂Cl₂–CH₃CN mixture. By contrast, its *cis* isomer **8a** underwent an exclusive Ar–N reductive elimination in the same solvent already at room temperature, but instead of the expected monoarylamines *n*-BuNHAr, **5a**, the diarylamines *n*-BuNAr₂, **6a**, was produced in 89% NMR yield, along with Pt(II) fluoro complexes **10–L** (Scheme 6, top).²⁰

Scheme 6. Ar–N(Alk) Bond Formation at a Pt(IV) Center



The identity of **6a** was confirmed by NMR spectroscopy and mass spectrometry. The C–N coupling of **8a** followed a first-order kinetics ($k_{298} = 3.7 \pm 0.5 \times 10^{-3} \text{ s}^{-1}$, $\Delta G^\ddagger = 23.5 \text{ kcal/mol}$). No intermediates were observed by ¹⁹F NMR spectroscopy.

Remarkably, only the monoarylated product **5a** was formed in 97% yield after 1 h of reaction of **8a** at 20 °C in the presence of 1 equiv of an external base, Et₃N (Scheme 6, bottom). No **6a** was observed under these conditions. Similar to the external base-free reaction leading to the diarylamines **6a**, the C–N

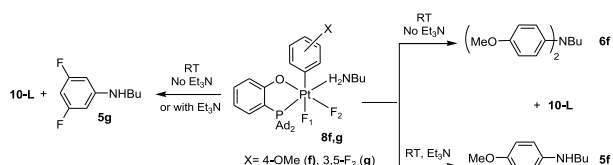
elimination of **8a** in the presence of 1 equiv. (0.013 mmol) of Et₃N to form the monoarylamines **5a** followed a first-order kinetics but roughly 10 times faster ($k_{298} = 4.9 \pm 0.7 \times 10^{-4} \text{ s}^{-1}$, $\Delta G^\ddagger = 21.9 \text{ kcal/mol}$, Figure S3). Thus, the external base accelerates the elimination of the monoarylamines **5a** from **8a**, thus making this reaction much faster than the subsequent arylation of **5a** by a second equivalent of **8a** and leaving the second arylation out of competition. The accelerating effect of Et₃N additives on the first arylation step and the absence of such an effect on the second arylation step is explained in subsections 2.5.4 and 2.5.5 in the Computational Studies section. Notably, with 2 equiv of Et₃N, the reaction of **8a** to form **5a** was even faster and was complete within 30 min at 25 °C.

Having analyzed the C–N coupling reactivity of the Pt(IV) *n*-butylamine aryl complex **8a**, we next looked at the reactivity of some analogous complexes (P–O)Pt^{IV}F₂(*p*-FC₆H₄)(NH₂Alk) containing other primary alkylamines as ligands, PhCH₂NH₂ (**8b**), *c*-C₆H₁₁NH₂ (**8c**), and *t*-BuNH₂ (**8d**). Similar to **8a**, complexes **8b** and **8c** also readily undergo double N-arylation in a 2:1 CH₂Cl₂/MeCN solution to form the derived (4-FC₆H₄N)₂Alk products **6b** and **6c** in 93% and 44% yields, respectively (Scheme 6). By contrast, the bulkier *t*-BuNH₂ derivative **8d** gives the monoarylated product **5d** only in a low 15% yield along with a number of unidentified byproducts. Hence, the increasing steric bulk of the primary alkylamine ligand used in this reaction, *n*-BuNH₂ \approx PhCH₂NH₂ < *c*-C₆H₁₁NH₂ < *t*-BuNH₂, appears to affect both the N-arylation selectivity, by disfavoring the formation of diarylated products, and the overall N-arylation efficiency, which also decreases in this direction. Notably, a cyclopropylmethylamine (*c*-C₃H₅CH₂NH₂) analogue **8e** reacts cleanly to form the diarylamines **6e** as the only organic product without the formation of any cyclopropane ring-opening products. These diarylation reactions are also not inhibited by 1 equiv of butylated hydroxytoluene (BHT), thus arguing against realization of a radical mechanism.

Similar to the *n*-butylamine complex **8a**, the presence of a Et₃N additive triggered the C–N coupling of the benzylamine adduct **8b** and the cyclohexylamine complex **8c** to produce selectively the derived monoarylamines **5b** (95%) and **5c** (98%), respectively, within 1.5 h at room temperature.¹⁷ For the *tert*-butylamine complex **8d**, the yield of the derived monoarylamines **5d** rose from 15% to ca. 50% in the presence of Et₃N. The identity of the organic products was confirmed by NMR spectroscopy, MS, and single-crystal X-ray diffraction analysis of 4-FC₆H₄NHCy–(P–O)Pt(II) derivative (**10–5c**, Scheme 6). Finally, the addition of equimolar amounts of *n*-BuNH₂ and Et₃N directly to the pyridine complex **1** leads to the formation of the monoarylamines **5a** in >90% NMR yield.

2.3. C–N Coupling Reactions Involving Various Pt(IV) Aryls. Having analyzed the reactivity trends related to the formation of monoarylamines **5** versus diarylamines **6** that we observed in the reactions of the respective Pt(IV) *p*-fluorophenyl complexes (P–O)Pt^{IV}F₂(Ar)(NH₂Alk), **8a–8d** (Ar = *p*-C₆H₄F), we decided to probe the effect of the aryl ligand Ar on these reactions. An electron-rich *p*-methoxyphenyl *n*-butylamine complex **8f** and an electron-poorer 3,5-difluorophenyl analogue, **8g**, have been prepared, and their C–N coupling reactivity has been characterized (Scheme 7). The *p*-methoxyphenyl complex **8f**, an electron-rich analogue of **8a**, showed a reactivity that is similar to that of **8a**. This complex reacted in a 2:1 CH₂Cl₂/MeCN solution

Scheme 7. Ar–N(Alk) Bond Formation Involving Various Ar Groups



at 20 °C to form the expected diarylation product *n*-BuN(4-MeOC₆H₄)₂, **6f**, as the only organic product, in the absence of an external base, and the monoarylation product *n*-BuNH(4-MeOC₆H₄), **5f**, in the presence of 1 equiv of Et₃N.

A different behavior was observed for the 3,5-difluorophenyl complex **8g**, an electron-poorer analogue of **8a** (Scheme 7). In this case, the monoarylamine *n*-BuNH(3,5-F₂C₆H₃), **5g**, was observed as the major product, both in the absence of an external base (54% NMR yield after 3 h at 45 °C) and in the presence of 1 equiv of Et₃N (97% NMR yield after 1 h at 20 °C). The distinct reactivity of **8g** and **8f** in N-arylation reactions will be discussed in subsection 2.5.6 of the Computational Studies section.

These results (Scheme 7) suggest that, in general, there is a delicate balance between the formation of *N*-monoarylamines **5** and their *N,N*-diaryl analogues **6**, which are produced in a parallel reaction between **5** and the second equivalent of the Pt(IV) aryl complex **8**. This balance is affected, besides the presence of Et₃N additives, by the identity of the aryl ligand in **8**. For example, when a monoaryllalkylamine PhNHMe, **5h**, was added to a solution of the 4-fluorophenyl complex **8a** (see the ¹⁹F NMR spectrum in Figure 1, top), the added amine was

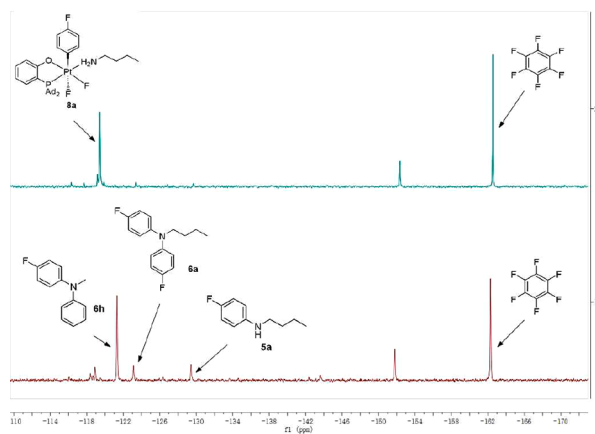


Figure 1. Fragments of ¹⁹F NMR spectra of the respective reaction mixtures, demonstrating a competitive arylation of monoarylamines PhNHMe, **5h**, and *p*-FC₆H₄NHⁿBu, **5a**, formed in situ: the starting complex **8a** (top) and a reaction mixture of **8a** and **5h** (bottom).

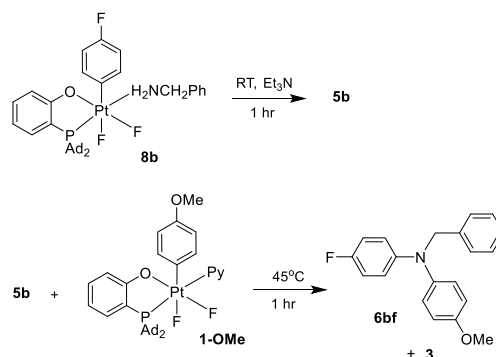
N-arylated and the derived product Ph(4-FC₆H₄)NMe, **6h**, formed in 73% NMR yield. Only small amounts of **5a** and **6a** were observed (Figure 1, bottom), resulting from a background reaction of **8a** (see Scheme 6). This result demonstrates that the intermolecular *N*-arylation of the free amine **5h** with **8a** is faster as compared to, formally, the intramolecular *N*-arylation of the coordinated *n*-butylamine amine ligand present in **8a**.

On the other hand, when the same monoaryllalkylamine **5h** was added to a solution of an electron-poorer Pt(IV) 3,5-

difluorophenyl complex **8g**, the intermolecular *N*-arylation of the added amine was barely noticeable, so that only a trace amount of the derived diarylamine Ph(3,5-F₂C₆H₃)NMe, **6h**, was observed. Here, the major reaction product was the monoarylamine **5g** that resulted from the intramolecular *N*-arylation of the coordinated *n*-butylamine ligand present in **8g** (Scheme 7, left). This result demonstrates that the intramolecular *N*-arylation of the *n*-butylamine ligand in **8g** is now faster than the intermolecular *N*-arylation of **5h** or **5g**.

As discussed in section 2.5.6, this change in the reaction selectivity compared to **8a** results from the electron-poorer Pt(IV) center in **8g** being slower to exchange its coordinated *n*-butylamine ligand for **5h** or **5g** in the step preceding *N*-arylation of these exogenous amines.

2.4. Some Applications of Pt(IV) Aryls for *N*-Arylation of Alkylamines and Protected Amino Acids. The ability of monoaryllalkylamines **5** to undergo second arylation with suitable Pt(IV) aryl complexes, **8** or **1** (vide supra), opens the possibility to generate unsymmetrically substituted *N*-Ar-*N*-Ar'-alkylamines in a stepwise manner under mild conditions. In support of this notion, the addition of **5b** to a solution of a *p*-methoxyphenyl pyridine Pt(IV) complex, **1-OMe** (Scheme 8),

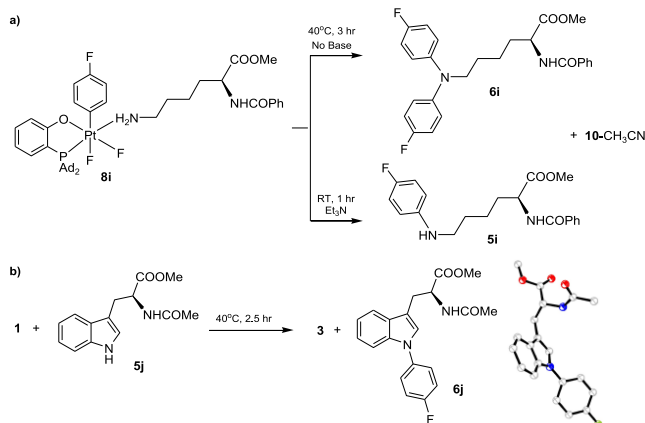
Scheme 8. One-Pot Synthesis of an Unsymmetrical Diarylamine **6bf**

led to the clean formation of the diaryllalkylamine **6bf** bearing two aryl groups of different electronic demand after 1 h at room temperature. Furthermore, two arylation reactions involving two different aryl Pt(IV) complexes can be performed sequentially without isolation of an intermediate monoarylamine **5**.

For example, reacting the *p*-fluorophenyl Pt(IV) complex **8b** in the presence of 1 equiv of Et₃N for 1 h followed by the addition of **1-OMe** resulted in a clean formation of **6bf** (97% yield, see Scheme 8).

A particularly interesting application of this new chemistry involves *N*-arylation of amino acid derivatives by (P–O)Pt(IV) aryl complexes. Recently, *N*-arylation of an amino acid has received a great deal of attention as a new technique for late-stage modification of peptides and proteins.²¹ In particular, an ϵ -NH₂ arylation of the lysine (Lys) residue was reported in selected oligopeptides using Pd(II) complexes under mild basic conditions.^{16e} In our system, the *p*-fluorophenyl Pt(IV) complex **8i**, bearing a partially protected Lys as a ligand, underwent facile di-*N*-arylation in the absence of external base additives, at 40 °C, to give **6i** as the only product in a 88% yield after 3 h. In the presence of Et₃N, the same reaction led to a selective monoarylation of a Lys side chain to give **5i** in a 93% yield (Scheme 9a), thus

Scheme 9. N-Arylation of Amino Acid Derivatives



demonstrating an easy-to-control selectivity in mono- and di-N-arylation of amino acid derivatives. Furthermore, the observed reactivity of a secondary amino group, such as in compounds **5**, led us to explore the N–H arylation of tryptophan (Trp), which has never been demonstrated under mild base-free conditions.^{22,23} Satisfyingly, the addition of a Trp derivative **5j** to a solution of **1** resulted in a clean formation of **6j** in a 91% NMR yield, which was characterized crystallographically (Scheme 9b).

2.5. Computational Studies of Aryl–X Coupling Reactions from Pt(IV). Unlike the commonly proposed S_N2 -type reductive elimination of $C(sp^3)$ –X bonds from $M(IV)$ –alkyl complexes,^{1–5,10,11} the aryl $C(sp^2)$ –X coupling of complexes **2** and **8** may be expected to occur as a concerted process.¹² To confirm the viability of such C–X coupling mechanism in these reactions, we carried out their computational modeling. In our calculations we utilized the density functional theory (DFT) method implemented in the *Jaguar* program package,²⁴ using the PBE functional²⁵ and LACVP relativistic basis set with two polarization functions. This level of theory was used successfully in previous works dealing with modeling of kinetics of organometallic reactions.^{8,26} A frequency analysis was performed for all stationary points. In addition, using the method of intrinsic reaction coordinate, reactants, products, and the corresponding transition states were proven to be connected by a single minimal energy reaction path. The solvation Gibbs energies in MeCN for all solutes were found using single-point calculations utilizing the Poisson–Boltzmann continuum solvation model, as implemented in the *Jaguar* package.²⁴

2.5.1. Aryl–CN Elimination of the Pt(IV) Cyano Complex 2a. The results of our analysis of elimination of p -FC₆H₄–CN, **4a**, from the aryl Pt(IV) cyano complex **2a** are presented in Figures 2 and 3. A concerted C–C coupling at a Pt(IV) center would require a cis arrangement of the aryl and CN ligands, which is not the case for complex **2a**. Hence, we considered a three-step reaction sequence (Figure 2) including (a) pyridine ligand loss to form a 5-coordinate transient **2aa** ($\Delta G^\circ_{298} = 11.1$ kcal/mol), (b) its *trans*-Ar, CN/*cis*-Ar, CN isomerization leading to **2ab** ($\Delta G^\circ_{298} = -1.4$ kcal/mol) having the Ar and CN ligands in the required cis position, and (c) the Ar–CN coupling of the transient **2ab**. Because the transition state $TS_d(2a)$ for the pyridine dissociation could not be found, we used the calculated reaction enthalpy for this step, 24.4 kcal/mol, as an upper estimate for its Gibbs activation energy. This approximation suggests that the entropy changes are small

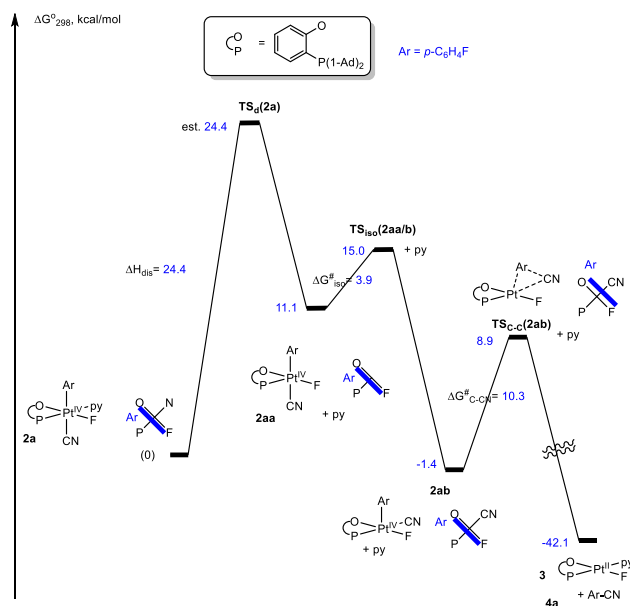


Figure 2. Reaction Gibbs energy profile for the C–CN bond elimination of p -FC₆H₄–CN, **4a**, from complex **2a** in MeCN solution. The energy of $TS_d(2a)$ is estimated.

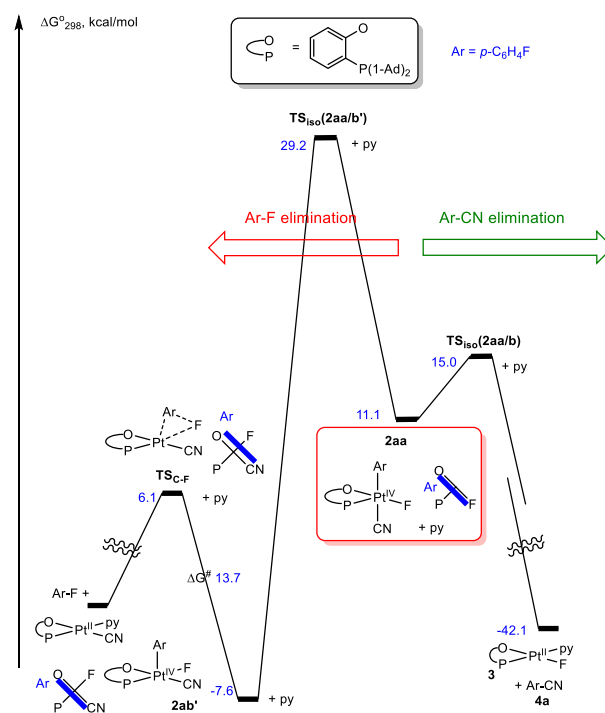


Figure 3. Reaction Gibbs energy profile for two diverging potentially competitive reaction paths of complex **2a** in MeCN solution involving five-coordinate intermediate **2aa** (see Figure 2): (a) the C–CN bond elimination to form p -FC₆H₄–CN, **4a** (right), see also Figure 2, and (b) the C–F bond elimination to form p -F₂C₆H₄ (left).

when going from **2a** to $TS_d(2a)$. The resulting 5-coordinate transient **2aa** undergoes a low-barrier ($\Delta G^\ddagger_{iso}(2aa/b) = 3.9$ kcal/mol) isomerization to **2ab**, which is involved in another low-barrier ($\Delta G^\ddagger_{C-CN}(2ab) = 10.3$ kcal/mol) C–C coupling step leading to product **4a** and the Pt(II) pyridine complex **3**. Overall, the pyridine dissociation is the rate-limiting step, and our estimate of the activation energy for this step, 24.4 kcal/

mol, is reasonably close to the observed reaction Gibbs activation energy of 26.9 kcal/mol.

Considering another plausible 5-coordinate intermediate, **2ab'** (Figure 3), having the fluoro ligand in place of the cyanide in **2ab**, we also checked how facile might be an Ar–F elimination of **2ab'**. Notably, **2ab'**, featuring the favorable arrangement of the fluoride and aryl ligands, can undergo C–F bond elimination to form 1,4-difluorobenzene with a low 13.7 kcal/mol Gibbs activation energy (Figure 3, left). Most importantly, in addition to being less competitive than the C–C coupling ($\Delta G^\ddagger_{\text{C-CN}} = 10.3$ kcal/mol), the isomerization of **2aa** to **2ab'** is characterized by a high 29.2 kcal/mol Gibbs activation energy (see also Figure S4 for an alternative isomerization path from **2aa** to **2ab'** with 28.9 kcal/mol Gibbs activation energy), thus making the isomer **2ab'** needed for the C–F coupling virtually inaccessible and the C–F coupling noncompetitive. This result is in accord with the lack of the experimental observation of 1,4-difluorobenzene among our reaction products.

2.5.2. Aryl–O Elimination of the Pt(IV) Phenoxide Complex 2b. A similar computational analysis of the C–O elimination of the ether product, *p*-FC₆H₄–O–*p*-C₆H₄NO₂, **4b**, from the aryl Pt(IV) *p*-nitrophenoxo complex **2b** (Figure 4)

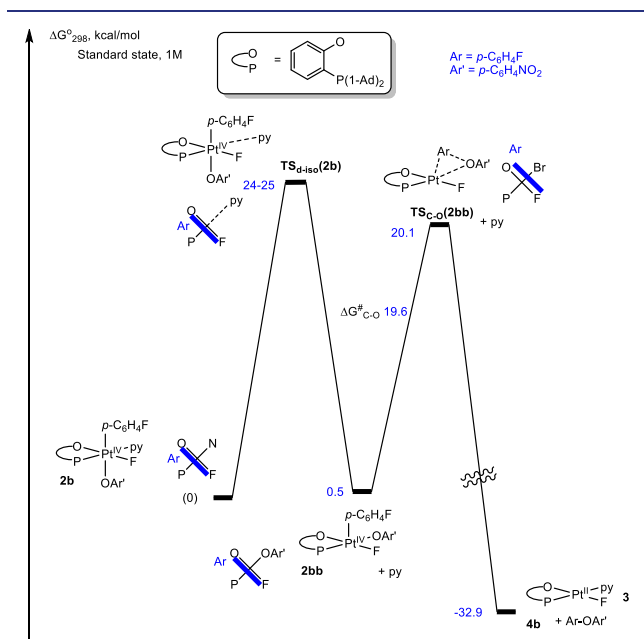


Figure 4. Reaction Gibbs energy profile for the C–O bond elimination of *p*-FC₆H₄–O–*p*-C₆H₄NO₂, **4b**, from complex **2b** in MeCN solution. The energy of $\text{TS}_{\text{d-iso}}(\mathbf{2b})$ is estimated.

shows the absence of any stable 5-coordinate species that would result from pyridine dissociation and would have trans arrangement of the Ar and O–*p*-C₆H₄NO₂ ligands. Our attempts to locate this structure on the potential energy surface led to its isomer **2bb** ($\Delta G^\circ_{298} = 0.5$ kcal/mol) with a cis arrangement of the Ar and O–*p*-C₆H₄NO₂ ligands. Hence, the pyridine ligand dissociation is accompanied by the change of the configuration of the Pt(IV) center. The resulting transient **2bb** undergoes facile C–O coupling with a Gibbs activation energy of 19.6 kcal/mol.

Our experimental data for the reaction rate constant, $k_{348} = (4.8 \pm 0.3) \times 10^{-5} \text{ s}^{-1}$ ($\Delta G^\ddagger_{348} = 27.3$ kcal/mol), show that the actual reaction Gibbs activation energy is greater than the

calculated 20.1 kcal/mol activation energy for the C–O coupling (Figure 4). Combined with the fact that no transients such as **2bb** were observed in the reaction, we presume that dissociation/5-coordinate transient isomerization step $\text{TS}_{\text{d-iso}}(\mathbf{2b})$ is rate-determining. The activation barrier for this step should be close to that for the reaction involving **2a**, 24–25 kcal/mol, which is a reasonably good match to the experimental value discussed.

2.5.3. Aryl–Cl Elimination of the Pt(IV) Chloro Complex 2c. The reaction Gibbs energy profile for the C–Cl coupling/elimination of *p*-FC₆H₄–Cl, **4c**, from the aryl Pt(IV) chloro complex **2c** (Figure S5) shows great similarity to that for complex **2b** (Figure 4). As for **2b**, a 5-coordinate transient with trans arrangement of the Ar and Cl ligands that is expected to result from pyridine ligand dissociation step could not be located, and its cis isomer **2cb** ($\Delta G^\circ_{298} = -0.4$ kcal/mol), an analogue of **2bb** in Figure 4, was the only derived 5-coordinate species that was found. The latter undergoes a facile C–Cl coupling with a Gibbs activation energy of 19.6 kcal/mol. The experimentally determined Gibbs activation energy for the C–Cl coupling, ΔG^\ddagger , is 23.3 kcal/mol. Similar to the case of **2b**, no intermediates were observed in this reaction, and we propose that the pyridine dissociation/5-coordinate transient isomerization step is rate-limiting here as well. We consider the expected barrier for this step to be about the same as that for **2a**, 24–25 kcal/mol, which is reasonably close to the experimental value of 23.2 kcal/mol.

2.5.4. Aryl–N Elimination of the Pt(IV) *n*-Butylamine Complex 8a in the Presence of Et₃N: *N*-Monoarylation. The most mechanistically intriguing, as compared to the C–X bond elimination of **2a**–**2c** (X = C, O, Cl), is the C–N coupling of the aryl Pt(IV) *n*-butylamine complex **8a** leading to either the monoarylamine *p*-FC₆H₄–NH*n*-Bu, **5a**, in the presence of Et₃N (Figure 5) or the diarylamine (*p*-FC₆H₄)₂N*n*Bu, **6a**, in the

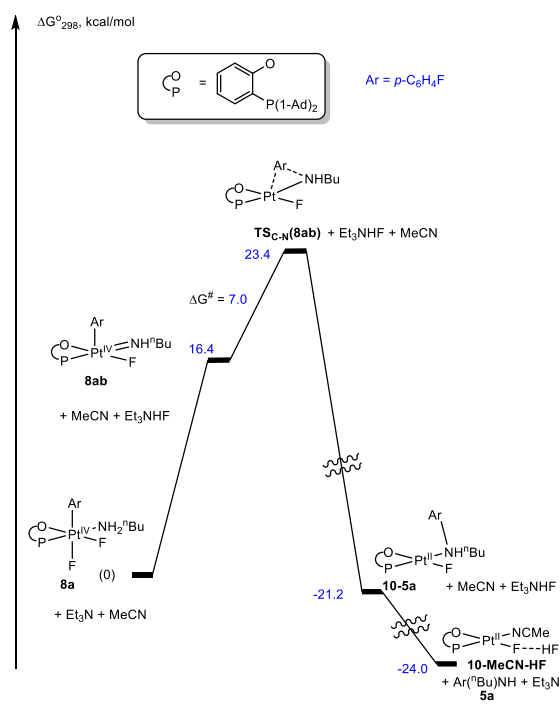


Figure 5. Reaction Gibbs energy profile for the C–N bond elimination of *p*-FC₆H₄–NH–*n*-Bu, **5a**, from complex **8a** in the presence of Et₃N in MeCN solution.

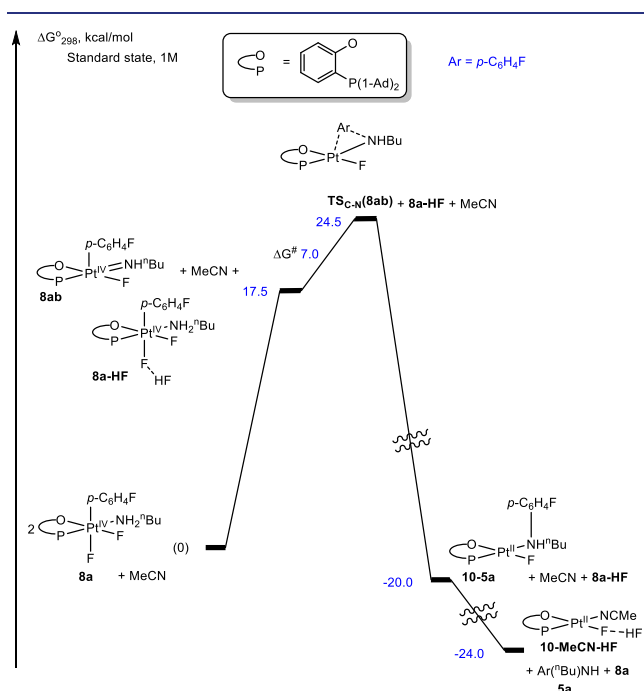


Figure 6. Reaction Gibbs energy profile for the first C–N coupling (first N-arylation) step of complex **8a** leading to *p*-FC₆H₄–NH–*n*-Bu, **5a**, in the absence of Et₃N in MeCN solutions.

absence of additives (Figures 6, 7, and S6). In **8a**, the amine and aryl ligands have the required *cis* arrangement, but the Gibbs activation energy corresponding to a direct C–N elimination of the ammonium cation *p*-FC₆H₄–NH₂⁺*n*Bu⁺ is too high, 33.2 kcal/mol (Figure S7). The most likely reaction mechanism (Figure 5) involves deprotonation of the coordinated amine with Et₃N leading overall to HF elimination from **8a** to produce a 5-coordinate Pt(IV) amido transient **8ab**. This step is endergonic ($\Delta G^\circ_{298} = 16.4$ kcal/mol), but the subsequent Ar–N coupling is facile with a Gibbs activation energy of only 7.0 kcal/mol.

The corresponding transition state TS_{C–N}(**8ab**) is the highest point on the reaction energy profile, and its energy, 23.4 kcal/mol, is a reasonable match to the experimentally determined Gibbs activation energy for the Et₃N-promoted C–N coupling, 21.9 kcal/mol. The resulting Pt(II) *N*-arylamine complex **10–5a** then can release free amine **5a** and form an acetonitrile adduct **10–MeCN** after ligand substitution with a MeCN solvent species. According to our calculations, the Pt(II) fluoride complex **10–MeCN** can form with HF a robust bifluoride derivative containing, formally, a HF₂[–] ligand. As a result, **10–MeCN** is a slightly stronger base, by 1.4 kcal/mol, with respect to HF, as compared to Et₃N, such that Et₃N can be viewed as an effective base catalyst for the amine monoarylation reaction.

2.5.5. *N,N*-Diarylation of *n*-Butylamine with **8a As the Arylating Agent in the Absence of Et₃N.** Two consecutive *N*-arylations of *n*-butylamine originating from complex **8a** to form *N,N*-diarylamine **6a** occur in the absence of Et₃N additives (Scheme 6, top). The first *N*-arylation in the absence (Figure 6) and presence of Et₃N (Figure 5) operates by a similar mechanism. In the absence of Et₃N, an HF elimination from **8a** to produce the 5-coordinate Pt(IV) amido transient **8ab** is

carried out by second equivalent of **8a**, acting as a Brønsted base, to form an ¹⁹F NMR-detectable bifluoride complex **8a–HF**. Notably, the Pt(IV) fluoro complex **8a** is a slightly weaker base than Et₃N. As a result, the HF-elimination step leading to **8ab** is 1.1 kcal/mol more endergonic in the absence of Et₃N, as compared to the reaction in the presence of Et₃N (Figure 5). Accordingly, the energy of the transition state TS_{C–N}(**8ab**) leading to the monoarylamine **5a** is now 1.1 kcal/mol higher, 24.5 kcal/mol (Figure 6). Finally, the HF produced in the first arylation step is transferred from **8a–HF** to the fluoride ligand of **10–MeCN** to form **10–MeCN–HF** and to release **8a** in a slightly exergonic reaction.

The second *N*-arylation reaction involves an initial **5a**-for-BuNH₂ substitution via a dissociative mechanism to form **8ac** (Figure 7), which is an *N*-(*n*-butyl)-*p*-fluoroaniline analogue of the *n*-butylamine complex **8a**. Remarkably, *N*-(*n*-butyl)-*p*-fluoroaniline **5a** is a worse ligand than *n*-butylamine, and the formation of **8ac** is a thermodynamically uphill process. However, the energy penalty for this step is diminished significantly because of the ability of the liberated *n*-butylamine to react exergonically with complex **10–MeCN–HF** by displacing its MeCN ligand via the transition state TS_{LS} (Figures 7 and S6).²⁰

A subsequent base-mediated reaction of **8ac** produces the five-coordinate Pt(IV) amido species featuring a bifluoride ligand, **8ad**. The HF transfer here may be mediated by **8a**. Finally, the platinum(IV) amido species **8ad** undergoes aryl–N reductive elimination with a low 4.8 kcal/mol barrier (TS_{C–N}(**8ad–HF**), Figure 7) to form the Pt(II) diarylamine complex **10–6a–HF**. The diarylamine **6a** is then liberated as a result of a ligand substitution with MeCN, along with the formation of **10–MeCN–HF**.

The highest energy points on the diagrams in Figures 6 and 7 corresponding to the first (Figure 6) and second (Figure 7) *N*-arylation reactions are 24.5 and 26.1 kcal/mol, respectively. Both values are reasonably close to the experimental Gibbs energy of activation for the overall *N,N*-diarylation reaction, 23.5 kcal/mol. The highest point for the second *N*-arylation, 26.1 kcal/mol, corresponding to *n*-butylamine ligand dissociation from complex **8a**, is approximated using the enthalpy change for the ligand dissociation and is likely overestimated. Finally, considering the whole reaction sequence involved in the second *N*-arylation (Figure 7), it is important to note that the substitution of *n*-butylamine ligand in **8a** with the incoming arylamine **5a** and the formation of **8ac** determine the rate of the whole *N*-arylation with either TS_d(**8a**) or TS_{LS} as the highest energy point on the reaction energy profile.

2.5.6. Use of Et₃N Additives to Control *N*-Mono- versus *N,N*-Diarylation Reactions Involving **8a, **8f**, and **8g**.** The mechanistic analysis presented in Figures 5–7 allows us to account for the remarkable effect of Et₃N additives on the C–N coupling reactivity of *n*-butylamine complex **8a**. The complex produces 0.5 equiv of *N,N*-diarylamine **6a** when no additives are present, whereas Et₃N additives trigger this reactivity so that **8a** selectively forms 1 equiv of *N*-monoarylamine **5a** (Scheme 6). As follows from the comparison of Figures 5 and 6, because it is a stronger base than **8a**, Et₃N accelerates the first C–N coupling step involving the coordinated *n*-butylamine and leading to **5a**. At the same time, Et₃N cannot accelerate the second intermolecular *N*-arylation leading to **6a** because the rate-determining step for the second *N*-arylation, the displacement of *n*-BuNH₂ from **8a** with *N*-arylamine **5a**, is unaffected by free Et₃N. This

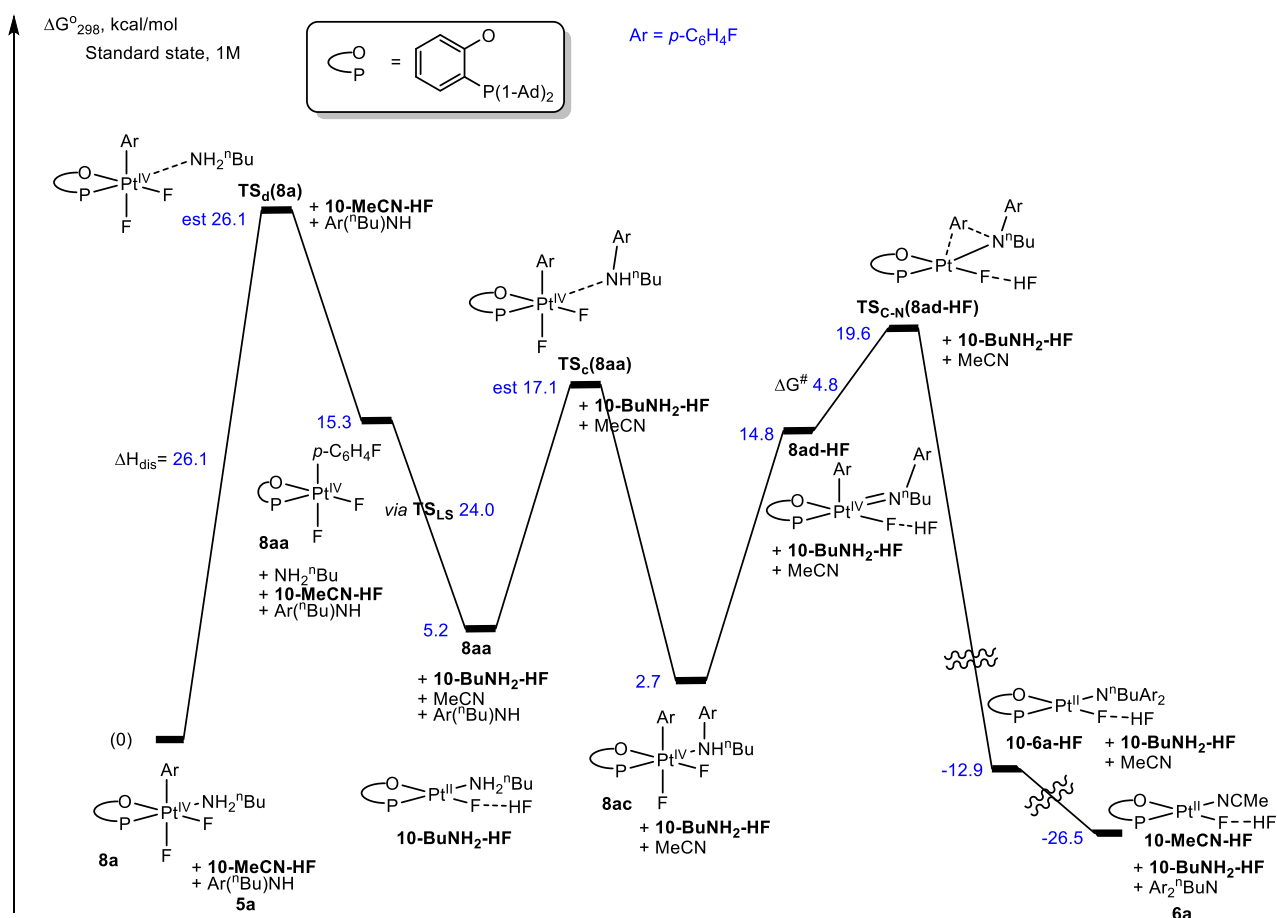


Figure 7. Gibbs energy profile for the second C–N coupling (second N-arylation) step of complex **8a** leading to (*p*-FC₆H₄)₂N-*n*-Bu, **6a**, in the absence of Et₃N in MeCN solution. The energies of TS_d(**8a**) and TS_s(**8aa**) are estimated.

mechanistic difference between the first and second N-arylation reactions results in the selective N-monoarylation of *n*-butylamine ligand when Et₃N is present.

Notably, the N-arylation reactivity of the electron-rich *p*-methoxyphenyl complex **8f** is similar to that of the *p*-fluorophenyl complex **8a**. For **8f**, the N,N-diarylation of the coordinated *n*-butylamine to produce **6f** (Scheme 7, right) is also facile in the absence of Et₃N, but, when Et₃N is available, only N-monoarylamines **5f** forms. However, the electron-poorer 3,5-difluorophenyl Pt(IV) complex **8g** produces exclusively N-monoarylamines **5g** (Scheme 7, left) in both the absence and the presence of Et₃N in the reaction mixture; the N,N-diarylation of coordinated *n*-butylamine is not observed.

This difference in the behavior of **8a**, **8g**, and **8f** can be accounted for by using the reaction mechanism proposed for the second N-arylation (Figure 7). According to our DFT calculations, the dissociation of coordinated *n*-butylamine is about as fast for **8f** as it is for **8a** with dissociation enthalpies of 26.0 versus 26.1 kcal/mol, respectively (Figure S8). In turn, for the electron-poorer complex **8g**, the ligand dissociation is predicted to be more endergonic, 26.9 kcal/mol. In support of the notion of the increasing Pt(IV)–(NH₂^{*n*}Bu) bond strength in the series of complexes **8f**, **8a**, and **8g**, which is related to the height of the amine dissociation barrier, two qualitative bond strength descriptors, the natural charge on the Pt(IV) atom and the natural localized orbital natural population analysis (NLMO/NPA) bond order for the Pt(IV)–N bond, were calculated. Both parameters were found to increase in the

order **8f** (electron-richest) < **8a** < **8g** (electron-poorest), thus suggesting a trend of the increasing Pt(IV)–N bond strength (Table 1).

Table 1. Natural Charge on the Pt(IV) Atom and the Pt(IV)–N NLMO/NPA Bond Order for the Pt(IV)–N Bond in *n*-Butylamine Complexes **8a**, **8f**, and **8g**

complex	natural charge on Pt(IV) atom	NLMO/NPA bond order for the Pt(IV)–N bond
8a	1.113	0.1654
8f	1.110	0.1649
8g	1.120	0.1662

To summarize, on the basis of the results above, in the absence of any better estimates for the Gibbs activation energy values for the *n*-BuNH₂ ligand dissociation step, we postulate that the slower rate of *n*-butylamine ligand substitution in **8g** leading to the key intermediate **8gc** is responsible for the reactivity change and the lack of the N,N-diarylated product.

3. CONCLUSIONS

In conclusion, we reported a series of facile aryl C(sp²)–X bond elimination reactions (X = Cl, CN, OAr, N(Alk)R) at a Pt(IV) center using a series of Pt(IV) aryl complexes of the same structural type. These reactions include C(sp²)–N coupling involving the Pt(IV)-coordinated aryl and primary alkylamine ligands. A combination of electronic properties and

steric bulk of the ancillary 2-[bis(adamant-1-yl)phosphino]-phenoxy ligand (P–O) appears to be an important factor governing this facile C–X bond-making chemistry. Interestingly, the isolated (P–O)Pt^{IV}F₂(Ar)(NH₂Alk) complexes undergo an unexpectedly facile double aryl C(sp²)–N coupling under mild conditions, giving diarylamines (Ar)₂NAlk in high yields (Ar = *p*-FC₆H₄, *p*-MeOC₆H₄). With the sterically demanding *t*-BuNH₂ or with the electron-poorer aryl ligand 3,5-F₂C₆H₃, only monoarylamines ArNHAlk are isolated under the same conditions. These results demonstrate the fine balance in the reactivity between the initially coordinated AlkNH₂ ligand and the product ArNHAlk resulting from the first C(sp²)–N coupling step. Importantly, in the presence of a base, such as Et₃N, all studied Pt(IV) complexes quantitatively give the corresponding monoarylamines ArNHAlk products within 1 h at room temperature. These findings allowed for a one-pot preparation of unsymmetrical diarylamines (Ar¹)-(Ar²)NAlk, all under mild conditions. The new chemistry was also successfully applied in the unprecedented arylation of two partially protected amino acids, resulting in a selective high-yielding single (with an added external base) or double (without external base additives) ϵ -NH₂-arylation of a lysine derivative and a high-yielding NH-arylation of a tryptophan derivative. Further studies on the reactivity of Pt(IV) complexes in the arylation of biologically relevant substrates are underway in our laboratories.

■ ASSOCIATED CONTENT

Supporting Information

The Supporting Information is available free of charge at <https://pubs.acs.org/doi/10.1021/jacs.0c09452>.

Experimental procedures, characterization, and spectroscopic data (PDF)

Computational data (PDF)

X-ray structural data (CIF)

■ AUTHOR INFORMATION

Corresponding Authors

Arkadi Vigalok – School of Chemistry, The Sackler Faculty of Exact Sciences, Tel Aviv University, Tel Aviv 69978, Israel; orcid.org/0000-0003-4097-0215; Email: avigal@tauex.tau.ac.il

Andrei N. Vedernikov – Department of Chemistry and Biochemistry, University of Maryland, College Park, Maryland 20742, United States; orcid.org/0000-0002-7371-793X; Email: avederni@umd.edu

Author

Xiaoxi Lin – School of Chemistry, The Sackler Faculty of Exact Sciences, Tel Aviv University, Tel Aviv 69978, Israel

Complete contact information is available at: <https://pubs.acs.org/doi/10.1021/jacs.0c09452>

Notes

The authors declare no competing financial interest.

■ ACKNOWLEDGMENTS

Dedicated to the memory of Professor Kilian Muñoz. This research was supported by a grant from the United States–Israel Binational Science Foundation (BSF), Jerusalem, Israel, and Joint NSFC–ISF Research Grant (2572/17). We are grateful to Prof. Guosheng Liu (Shanghai Institute of Organic

Chemistry) for a valuable discussion. We also thank Dr. Sophia Lipstman for performing the X-ray crystallographic analysis.

■ REFERENCES

- (1) (a) Racowski, J. M.; Sanford, M. S. Carbon-Heteroatom Bond-Forming Reductive Elimination from Palladium(IV) Complexes. *Top. Organomet. Chem.* **2011**, *35*, 61–84. (b) Vedernikov, A. N. Pd^{II}/Pd^{IV} Redox Couple Mediated C–X Bond Formation. *RSC Catalysis Series* **2013**, *11*, 108–121. (c) Camasso, N. M.; Sanford, M. S. Design, Synthesis and Carbon-Heteroatom Coupling Reactions of Organometallic Nickel(IV) Complexes. *Science* **2015**, *347*, 1218–1220.
- (2) (a) Muniz, K. High-Oxidation-State Palladium Catalysis: New Reactivity for Organic Synthesis. *Angew. Chem., Int. Ed.* **2009**, *48*, 9412–9423. (b) Desnoyer, A. N.; Love, J. A. Recent Advances in Well-Defined, Late Transition Metal Complexes That Make and/or Break C–N, C–O and C–S Bonds. *Chem. Soc. Rev.* **2017**, *46*, 197–238.
- (3) Vigalok, A. Electrophilic Halogenation–Reductive Elimination Chemistry of Organopalladium and -Platinum Complexes. *Acc. Chem. Res.* **2015**, *48*, 238–247.
- (4) Pérez-Temprano, M. H.; Racowski, J. M.; Kampf, J. W.; Sanford, M. S. Competition between sp³-C–N vs sp³-C–F Reductive Elimination from Pd^{IV} Complexes. *J. Am. Chem. Soc.* **2014**, *136*, 4097–4100. (b) Pendleton, I. M.; Pérez-Temprano, M. H.; Sanford, M. S.; Zimmerman, P. M. C Experimental and Computational Assessment of Reactivity and Mechanism in C(sp³)–N Bond-Forming Reductive Elimination from Palladium(IV). *J. Am. Chem. Soc.* **2016**, *138*, 6049–6060.
- (5) (a) Racowski, J. M.; Gary, J. B.; Sanford, M. S. Carbon(sp³)-Fluorine Bond-Forming Reductive Elimination from Palladium(IV) Complexes. *Angew. Chem., Int. Ed.* **2012**, *51*, 3414–3417. (b) Crosby, S. H.; Thomas, H. R.; Clarkson, G. J.; Rourke, J. P. Concerted Reductive Coupling of an Alkyl Chloride at Pt(IV). *Chem. Commun.* **2012**, *48*, 5775–5777.
- (6) For recent reviews, see: (a) Testa, C.; Roger, J.; Fleurat-Lessard, P.; Hierro, J.-C. Palladium-Catalyzed Electrophilic C–H-Bond Fluorination: Mechanistic Overview and Supporting Evidence. *Eur. J. Org. Chem.* **2019**, *2019*, 233–253. (b) Timsina, Y. N.; Gupton, B. F.; Ellis, K. C. Palladium-Catalyzed C–H Amination of C(sp²) and C(sp³)–H Bonds: Mechanism and Scope for N-Based Molecule Synthesis. *ACS Catal.* **2018**, *8*, 5732–5776. (c) Le Bras, J.; Muzart, J. Dehydrogenative (Hetero)arene Alkoxylation Triggered by Pd^{II}Catalyzed C(sp²)–H Activation and Coordinating Substituent: Pd^{II,III} or Pd^{IV} Complex as Key Intermediate? *Eur. J. Org. Chem.* **2017**, *2017*, 3528–3548. (d) Petrone, D. A.; Ye, J.; Lautens, M. Modern Transition-Metal-Catalyzed Carbon–Halogen Bond Formation. *Chem. Rev.* **2016**, *116*, 8003–8104. For earlier reviews, see: (e) Dick, A. R.; Sanford, M. S. Transition Metal Catalyzed Oxidative Functionalization of Carbon–Hydrogen Bonds. *Tetrahedron* **2006**, *62*, 2439–2463. (f) Muñoz, K.; Hövelmann, C. H.; Streuff, J.; Campos-Gómez, E. First Palladium- and Nickel-Catalyzed Oxidative Diamination of Alkenes: Cyclic Urea, Sulfamide, and Guanidine Building Blocks. *Pure Appl. Chem.* **2008**, *80*, 1089–1096. (g) Vigalok, A. Metal-Mediated Formation of Carbon–Halogen Bonds. *Chem. - Eur. J.* **2008**, *14*, 5102–5108. (h) Giri, R.; Shi, B.-F.; Engle, K. M.; Maugel, N.; Yu, J.-Q. Transition Metal-Catalyzed C–H Activation Reactions: Diastereoselectivity and Enantioselectivity. *Chem. Soc. Rev.* **2009**, *38*, 3242–3272.
- (7) For a rare example of Pt^{II/IV}-mediated oxidative C–H arylation, see (a) Wagner, A. M.; Hickman, A. J.; Sanford, M. S. Platinum-Catalyzed C–H Arylation of Simple Arenes. *J. Am. Chem. Soc.* **2013**, *135*, 15710–15713. For a catalytic C(sp³)–F bond formation using a Pt^{II/IV} cycle, see: (b) Cochrane, N. A.; Nguyen, H.; Gagne, M. R. Catalytic Enantioselective Cyclization and C3-Fluorination of Polyenes. *J. Am. Chem. Soc.* **2013**, *135*, 628–631.
- (8) Dubinsky-Davidchik, I. S.; Goldberg, I.; Vigalok, A.; Vedernikov, A. N. Selective Aryl–Fluoride Reductive Elimination from a Platinum(IV) Complex. *Angew. Chem., Int. Ed.* **2015**, *54*, 12447–12451.

- (9) (a) Yahav-Levi, A.; Goldberg, I.; Vigalok, A.; Vedernikov, A. N. Competitive Aryl-Iodide vs Aryl-Aryl Reductive Elimination Reactions in Pt(IV) Complexes: Experimental and Theoretical Studies. *J. Am. Chem. Soc.* **2008**, *130*, 724–731. (b) Yahav-Levi, A.; Goldberg, I.; Vigalok, A.; Vedernikov, A. N. Aryl-Bromide Reductive Elimination from an Isolated Pt(IV) Complex. *Chem. Commun.* **2010**, *46*, 3324–3326. (c) Kaspi, A. W.; Goldberg, I.; Vigalok, A. Reagent-Dependent Formation of C–C and C–F Bonds in Pt Complexes: An Unexpected Twist in the Electrophilic Fluorination Chemistry. *J. Am. Chem. Soc.* **2010**, *132*, 10626–10627. (d) Dubinsky-Davidchik, I. S.; Goldberg, I.; Vigalok, A.; Vedernikov, A. N. Unprecedented 1,3-Migration of the Aryl Ligand in Metallocyclic aryl α -Naphthyl Pt(IV) Difluorides to Produce β -Arylnaphthyl Pt(II) Complexes. *Chem. Commun.* **2013**, *49*, 3446–3448.
- (10) (a) Khusnutdinova, J. R.; Zavalij, P. Y.; Vedernikov, A. N. C–O Coupling of $\text{LPt}^{\text{IV}}\text{Me}(\text{OH})\text{X}$ Complexes in Water ($\text{X} = ^{18}\text{OH}, \text{OH}, \text{OMe}$; $\text{L} = \text{Di}(2\text{-pyridyl})\text{methane Sulfonate}$). *Organometallics* **2007**, *26*, 3466–3483. (b) Khusnutdinova, J. R.; Newman, L.; Zavalij, P. Y.; Lam, Y.-F.; Vedernikov, A. N. Direct $\text{C}(\text{sp}^3)\text{--O}$ Reductive Elimination of Olefin Oxides from Pt^{IV} -Oxetanes Prepared by Aerobic Oxidation of Pt^{II} Olefin Derivatives (Olefin = *cis*-Cyclooctene, Norbornene). *J. Am. Chem. Soc.* **2008**, *130*, 2174–2175. (c) Adams, D. J.; Johns, B.; Vedernikov, A. N. Methyl Transfer Reactivity of Pentachloromethylplatinate(IV) Anion with a Series of N-Nucleophiles. *J. Organomet. Chem.* **2019**, *880*, 22–28.
- (11) (a) Luinstra, G. A.; Labinger, J. A.; Bercaw, J. E. Mechanism and Stereochemistry for Nucleophilic Attack at Carbon of Platinum(IV) Alkyls: Model Reactions for Hydrocarbon Oxidation with Aqueous Platinum Chlorides. *J. Am. Chem. Soc.* **1993**, *115*, 3004–3005. (b) Williams, B. S.; Goldberg, K. I. Studies of Reductive Elimination Reactions To Form Carbon-Oxygen Bonds from Pt(IV) Complexes. *J. Am. Chem. Soc.* **2001**, *123*, 2576–2587. (c) Smythe, N. A.; Grice, K. A.; Williams, B. S.; Goldberg, K. I. Reductive Elimination and Dissociative β -Hydride Abstraction from Pt(IV) Hydroxide and Methoxide Complexes. *Organometallics* **2009**, *28*, 277–288. (d) Pawlikowski, A. V.; Getty, A. D.; Goldberg, K. I. Alkyl Carbon-Nitrogen Reductive Elimination from Platinum(IV)-Sulfonamide Complexes. *J. Am. Chem. Soc.* **2007**, *129*, 10382–10393.
- (12) (a) Vigalok, A. Late Transition Metal-Mediated Formation of Carbon–Halogen Bonds. In *Topics in Organometallic Chemistry*; Vigalok, A., Ed.; Springer: 2010; Vol. 31 (C–X Bond Formation), pp 19–38. (b) Vedernikov, A. N. C–O Reductive Elimination from High Valent Pt and Pd Centers. In *Topics in Organometallic Chemistry*; Vigalok, A., Ed.; Springer: 2010; Vol. 31 (C–X Bond Formation), pp 101–121.
- (13) Iglesias, A.; Muniz, K. Studies on Alkyl-Nitrogen Bond Formation via Reductive Elimination from Monomeric Palladium Complexes in High Oxidation State. *Helv. Chim. Acta* **2012**, *95*, 2007–2025.
- (14) For a pyridine nucleophile in a Pt(IV) system, see: (a) Rivada-Whealaghan, O.; Roselló-Merino, M.; Diez, J.; Maya, C.; López-Serrano, J.; Conejero, S. Formation of C–X Bonds through Stable Low-Electron-Count Cationic Platinum(IV) Alkyl Complexes Stabilized by N-Heterocyclic Carbenes. *Organometallics* **2014**, *33*, 5944–5947. For a relevant phosphine nucleophile, see: (b) Traversa, E.; Templeton, J. L.; Cheng, H. Y.; Mohadjer Beromi, M.; White, P. S.; West, N. M. Reductive Elimination from Platinum(IV) Aminotroponimate Dimethyl Complexes Promoted by Sterically Hindered Lewis Bases. *Organometallics* **2013**, *32*, 1938–1950. An $\text{S}_{\text{N}}2$ reaction in a Rh(III)–Me with alkylamine as the nucleophile was reported: (c) Stevens, T. E.; Smoll, K. A.; Goldberg, K. I. Direct Formation of Carbon(sp^3)–Heteroatom Bonds from Rh^{III} To Produce Methyl Iodide, Thioethers, and Alkylamines. *J. Am. Chem. Soc.* **2017**, *139*, 7725–7728.
- (15) Abada, E.; Zavalij, P. Y.; Vedernikov, A. N. Reductive $\text{C}(\text{sp}^2)\text{--N}$ Elimination from Isolated Pd(IV) Amido Aryl Complexes Prepared Using H_2O_2 as Oxidant. *J. Am. Chem. Soc.* **2017**, *139*, 643–646.
- (16) (a) Hartwig, J. F. In *Handbook of Organopalladium Chemistry for Organic Synthesis*; Negishi, E. I., Ed.; Wiley-Interscience: New York, 2002; Vol. 1, pp 1051–1058. (b) Hartwig, J. F. *The Organotransition Metal Chemistry: From Bonding to Catalysis*; University Science Books: Sausalito, CA, 2010. (c) Buchwald, S. L.; Mauger, C.; Mignani, G.; Scholz, U. Industrial-Scale Palladium-Catalyzed Coupling of Aryl Halides and Amines – A Personal Account. *Adv. Synth. Catal.* **2006**, *348*, 23–39. (d) Ruiz-Castillo, P.; Buchwald, S. L. Applications of Palladium-Catalyzed C–N Cross-Coupling Reactions. *Chem. Rev.* **2016**, *116*, 12564–12649. (e) Lee, H. G.; Lautrette, G.; Pentelute, B. L.; Buchwald, S. L. Palladium-Mediated Arylation of Lysine in Unprotected Peptides. *Angew. Chem., Int. Ed.* **2017**, *56*, 3177–3181.
- (17) (a) Ghosh, A.; Sieser, J. E.; Caron, S.; Watson, T. J. N. Synthesis of the κ -Agonist CJ-15,161 via a Palladium-Catalyzed Cross-Coupling Reaction. *Chem. Commun.* **2002**, 1644–1645. (b) Gudmundsson, K. S.; Johns, B. A. Synthesis of Novel Imidazo[1,2-a]pyridines with Potent Activity against Herpesviruses. *Org. Lett.* **2003**, *5*, 1369–1372. (c) Senten, K.; Van der Veken, P.; De Meester, I.; Lambeir, A. M.; Scharpe, S.; Haemers, A.; Augustyns, K. γ -Amino-Substituted Analogues of 1-[(S)-2,4-Diaminobutanoyl]-piperidine as Highly Potent and Selective Dipeptidyl Peptidase II Inhibitors. *J. Med. Chem.* **2004**, *47*, 2906–2916.
- (18) See Supporting Information for details.
- (19) The 21% yield is calculated based on the amount of the starting material; that corresponds to 42% if the aryl group balance is considered.
- (20) The eliminated amines $4\text{-FC}_6\text{H}_4\text{NHAlk}$ as well as RNH_2 , along with CH_3CN , are involved in coordination with Pt(II), as demonstrated by an example of an isolated adduct **10–5c** (Scheme 6). The formation of a mixture of the derived Pt(II) fluoro complexes **10–L** is supported by the ^{19}F NMR spectroscopy. The fluoro complexes **10–L** may also exist as bifluorides $(\text{P–O})\text{Pt}(\text{L})(\text{F–HF})$, as evidenced by occasional observation of a signal at ~ -180 ppm in the ^{19}F NMR spectra. To liberate the free amines and obtain more accurate integration ratios, reaction mixtures were treated with excess pyridine, resulting in the formation of a Pt(II) pyridine adduct **3**.
- (21) (a) Zhang, C.; Vinogradova, E. V.; Spokoyny, A. M.; Buchwald, S. L.; Pentelute, B. L. Arylation Chemistry for Bioconjugation. *Angew. Chem., Int. Ed.* **2019**, *58*, 4810–4839. (b) Bisseret, P.; Abdelkafi, H.; Blanchard, N. Aryl Transition Metal Chemical Warheads for Protein Bioconjugation. *Chem. Sci.* **2018**, *9*, 5132–5144. (c) Jbara, M.; Maity, S. K.; Brik, A. Palladium in the Chemical Synthesis and Modification of Proteins. *Angew. Chem., Int. Ed.* **2017**, *56*, 10644–10655.
- (22) Gruß, H.; Sewald, N. Late-Stage Diversification of Tryptophan-Derived Biomolecules. *Chem. - Eur. J.* **2020**, *26*, 5328–5340.
- (23) (a) Alonso, I.; Alvarez, R.; de Lera, A. R. Indole–Indole Ullmann Cross-Coupling for $\text{C}_{\text{Ar}}\text{--N}$ Bond Formation: Total Synthesis of (–)-Aspergilazine A. *Eur. J. Org. Chem.* **2017**, *2017*, 4948–4954. (b) Chapman, C. J.; Matsuno, A.; Frost, C. G.; Willis, M. C. Site-Selective Modification of Peptides Using Rhodium and Palladium Catalysis: Complementary Electrophilic and Nucleophilic Arylation. *Chem. Commun.* **2007**, 3903–3905. (c) Ma, F.; Xie, X.; Ding, L.; Gao, J.; Zhang, Z. Palladium-Catalyzed Coupling Reaction of Amino Acids (Esters) with Aryl Bromides and Chlorides. *Tetrahedron* **2011**, *67*, 9405–9410.
- (24) *Jaguar*, version 8.4; Schrödinger, LLC: New York, 2014.
- (25) Perdew, J. P.; Burke, K.; Ernzerhof, M. Generalized gradient approximation made simple. *Phys. Rev. Lett.* **1996**, *77*, 3865–3868.
- (26) (a) Hopmann, K. H. How Accurate is DFT for Iridium-Mediated Chemistry? *Organometallics* **2016**, *35*, 3795–3807. (b) Adams, D. J.; Johns, B.; Vedernikov, A. N. Methyl Transfer Reactivity of Pentachloromethylplatinate(IV) Anion with a Series of N-nucleophiles. *J. Organomet. Chem.* **2019**, *880*, 22–28.